Theor. Comput. Fluid Dyn. (2010) 24:349–361
DOI 10.1007/s00162-009-0146-1

SPECIAL ISSUE ORIGINAL ARTICLE

Stéphane Le Dizès · David Fabre

Viscous ring modes in vortices with axial jet

Received: 8 January 2009 / Accepted: 24 June 2009 / Published online: 11 August 2009

Abstract In this paper, we show the existence of new families of linear eigenmodes in vortices with axial jet. These modes are viscous in nature and concentrated in a ring around the vortex at the critical radial location $r_c > 0$ where $m\Omega_c' + kW_c' = 0$ where Ω_c' and W_c' are the radial derivative at r_c of the angular and axial velocity of the vortex. Using a large Reynolds-number asymptotic approach for an arbitrary axisymmetrical vortex with axial flow, both the complex frequency and the spatial structure of the eigenmodes are obtained for any azimuthal and axial wave number. The asymptotic predictions are compared to numerical results for the q-vortex and a good agreement is demonstrated. We show that for sufficiently large Reynolds numbers, a necessary and sufficient condition of instability of viscous ring modes is that there exists a location r_c where $\Omega_c\Omega_c'[r_c\Omega_c'(2\Omega_c + r_c\Omega_c') + (W_c')^2] < 0$ and $W_c' \neq 0$, which also corresponds to the condition of inviscid instability obtained by Leibovich and Stewartson (J Fluid Mech 126:335–356, 1983).

Keywords Vortex · Swirling jet · Instability · Viscosity · Breakdown · q-vortex · Ring mode

PACS 47.15.Fe, 47.20.Gv, 47.32.Cd

1 Introduction

Vortex stability is a domain of research as old as the general field of vortex dynamics. But, despite the enormous amount of works, the linear stability properties of simple vortices as the q-vortex model are still not fully known. For a long time, it has been believed that the q vortex was stable for swirl number q above 1.5 [1]. Recently, it was shown that not only inviscidly unstable modes exist up to $q \approx 2.35$ [5], but unstable viscous center modes exist whatever the a swirl number if the Reynolds number is sufficiently large [3,6]. It was demonstrated in [4,6] that these unstable viscous modes are generic perturbations in vortices with axial jet. Far from the marginal stability curves, they have a complicated multi-layered structure localized in an $O(Re^{-1/6})$ neighborhood of the vortex center, and a growth rate of the form $\sigma \sim \sigma_0 Re^{-1/3}$ where σ_0 is a simple function of the vortex parameters at the center [6,9]. The modes that will be described in this paper will be very similar in nature to these center modes. But, instead of being localized near the center, they will

Communicated by H. Aref

S. Le Dizès (✉)
Institut de Recherche sur les Phénomènes Hors Équilibre, CNRS & Aix-Marseille Université,
49, rue F. Joliot-Curie, B.P. 146, 13384 Marseille cedex 13, France
E-mail: ledizes@irphe.univ-mrs.fr

D. Fabre
Institut de Mécanique des Fluides de Toulouse, allée du Prof. Soula, 31400 Toulouse, France

be spatially concentrated near a particular radius corresponding to a double critical point of the inviscid equations. The mode structure will then form a cylindrical ring around the vortex. We shall provide the asymptotic structure of these ring modes in the limit of large Reynolds numbers.

Ring modes have already been obtained in an inviscid framework. Leibovich and Stewartson [7] and Stewartson [8] have been able to construct unstable ring modes by performing an asymptotic analysis in the limit of large azimuthal wave numbers m. Interestingly, the modes were also found to be localized near the double critical point mentioned above and the sufficient condition of instability which was derived [7] will turn out to be also a sufficient condition of instability of viscous ring modes.

The paper is organised as follows. In Sect. 2, the framework of the analysis is presented. Section 3 is concerned with the asymptotic analysis. The solutions in the different regions around the double critical point are obtained and matched in order to obtain the characteristics of the ring modes. An approximation for the most unstable ring modes and a general instability criterion are obtained in Sect. 4. In Sect. 5, the results are applied to the q-vortex model. We demonstrate that both the frequency and the spatial structure of the most unstable ring modes obtained by numerical integration are well predicted by the theory. The main results are then summarized in the last section.

2 Basic flow characteristics and perturbation equations

As in LDF07 [6], we consider a general axisymmetrical vortex with axial flow whose velocity field in cylindrical coordinates is

$$\mathbf{U}(r) = (0, V(r), W(r)), \tag{1}$$

where $V(r)$ and $W(r)$ are the azimuthal and the axial velocity respectively. We also define the angular velocity $\Omega(r)$ and the axial vorticity $\Xi(r)$ of this flow:

$$\Omega(r) = \frac{V(r)}{r}, \quad \Xi(r) = \frac{1}{r}\frac{d(rV)}{dr}. \tag{2}$$

The flow is assumed unbounded and the viscous diffusion of the base flow is neglected. However, the viscous effects on the perturbations which are responsible for the instability are considered. This is possible because the growth time scale of the unstable modes will be of order $Re^{1/3}$, that is smaller than the time scale $O(Re^{1/2})$ associated with the viscous diffusion of the basic flow.

Perturbations are searched in the form of normal modes

$$(\mathbf{U}, P) = (u, v, w, p)\mathrm{e}^{ikz+im\theta-i\omega t}, \tag{3}$$

where k and m are axial and azimuthal wave numbers and ω is the frequency. Inserting these expressions in the Navier-Stokes equations leads to the following linear system for the velocity and pressure amplitudes (u, v, w, p):

$$i\Phi u - 2\Omega v = -\frac{\partial p}{\partial r} + \frac{1}{Re}\left(\Delta u - \frac{u}{r^2} + \frac{2imv}{r^2}\right), \tag{4}$$

$$i\Phi v + \Xi u = -\frac{imp}{r} + \frac{1}{Re}\left(\Delta v - \frac{v}{r^2} - \frac{2imu}{r^2}\right), \tag{5}$$

$$i\Phi w + W'w = -ikp + \frac{1}{Re}\Delta w, \tag{6}$$

$$\frac{1}{r}\frac{\partial(ru)}{\partial r} + \frac{imv}{r} + ikw = 0, \tag{7}$$

where the prime denotes the derivative with respect to r, $\Delta = \partial_r^2 + (1/r)\partial_r - m^2/r^2 - k^2$ is the Laplacian operator, and $\Phi(r) = -\omega + m\Omega(r) + kW(r)$.

Perturbation amplitudes are also subject to boundary conditions: they must vanish at infinity and be bounded at the origin. The Reynolds number Re is constructed using the characteristic scales of the basic flow. Our goal is here to carried out an asymptotic analysis as $Re \to \infty$.

3 Asymptotic analysis and matching

3.1 Overview of the analysis

In LDF07, the existence of viscous modes localized in the center of the vortex was demonstrated. The frequency of these modes was shown to be at leading order $\omega \sim m\Omega(0)+kW(0)$. Moreover, owing to the peculiar properties of the vortex center which always satisfies $\Omega'(0) = W'(0) = 0$, the origin was also a double critical point for these modes.

Here, we shall show that the condition of existence of a double critical point r_c ($\neq 0$) is sufficient to form a viscous eigenmode. As for viscous center modes, we shall demonstrate that there exist families of eigenmodes whose frequency expands in the limit $Re \to \infty$ as

$$\omega \sim \omega_0 + Re^{-1/3}\omega_1 + Re^{-1/2}\omega_2 + \cdots \tag{8}$$

where

$$\omega_0 = m\Omega_c + kW_c, \quad m\Omega_c' + kW_c' = 0. \tag{9}$$

In the above equations, the subscript c indicates values taken at r_c and the primes derivatives with respect to the radial coordinate.

The existence of a double critical point different from the origin is not guaranteed for all profiles. For example, for a vortex without jet it requires $\Omega_c' = 0$ that is an extremum of the angular velocity at a non-zero radial location. The structure of the viscous ring modes will be as described in Fig. 1. There are important similarities between ring modes and center modes. As for center modes, in the Outer region the solution is non-viscous and possesses an essential singularity at the critical point r_c which requires the presence of a large $O(Re^{-1/6})$ layer around r_c to be smoothed. A similar $O(Re^{-1/4})$ layer (corresponding to an intermediate layer for the center modes) is also present for ring modes: it is in that region that eigenmodes are discretized. However, contrarily to center modes, ring modes are perfectly regular within the Intermediate region so no $O(Re^{-1/3})$ layer (Inner region) is needed.

The analysis given below follows in large part the presentation of LDF07. The reader can refer to this paper for details. As in LDF07, the matching between the solutions in the different regions is performed by using the pressure amplitude.

3.2 Outer Non-Viscous regions (ONV$^{\pm}$)

In the ONV$^{\pm}$ regions, the solution is assumed to be non-viscous at leading order. The pressure amplitude of the ONV$^{\pm}$ solution satisfies at leading order

$$\frac{d^2p_0}{dr^2} + \left(\frac{1}{r} - \frac{\Lambda'}{\Lambda}\right)\frac{dp_0}{dr} + \left(\frac{2m}{r\Phi^{(0)}\Lambda}(\Omega'\Lambda - \Omega\Lambda') + \frac{k^2\Lambda}{(\Phi^{(0)})^2} - \frac{m^2}{r^2} - \frac{2mkW'\Omega}{r(\Phi^{(0)})^2}\right)p_0 = 0, \tag{10}$$

where

$$\Phi^{(0)}(r) = -\omega_0 + m\Omega(r) + kW(r), \quad \Lambda(r) = 2\Xi(r)\Omega(r) - (\Phi^{(0)}(r))^2. \tag{11}$$

Because $\Phi^{(0)}(r_c) = 0$ and $\partial_r\Phi^{(0)}(r_c) = 0$, the solutions of (10) possess an essential singularity at r_c. Two independent solutions $p_0^{(1)}$ and $p_0^{(2)}$ can be chosen such that they behave near the critical point r_c as

$$p_0^{(1)} \sim |r - r_c|^{1/2}\exp\left(\frac{\beta}{|r - r_c|}\right), \quad p_0^{(2)} \sim |r - r_c|^{1/2}\exp\left(-\frac{\beta}{|r - r_c|}\right), \tag{12}$$

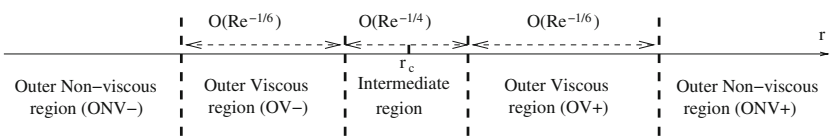

Fig. 1 Asymptotic structure of viscous ring modes

with

$$\beta = 2\frac{\sqrt{-H_c}}{K_c} \quad \text{such that} \quad -\pi/2 < \arg(\beta) \leq \pi/2, \tag{13}$$

where

$$H_c = 2\Omega_c k\left(\omega_c k - m\frac{W_c'}{r_c}\right), \quad K_c = \Phi_c^{(0)''} = m\Omega_c'' + kW_c''. \tag{14}$$

In each $ONV^{\pm}$ region, the solution to (10) is therefore a combination

$$p^{\pm} \sim A_\infty^{\pm} p_0^{(1)} + B_\infty^{\pm} p_0^{(2)}, \tag{15}$$

where $A_\infty^{\pm}$ and $B_\infty^{\pm}$ are $O(1)$ constants. As the solution can be multiplied by any amplitude factor, the only important numbers are the ratios $K^- = A_\infty^-/B_\infty^-$ and $K^+ = A_\infty^+/B_\infty^+$ which depend on the integration of (10) from 0 to r_c and from $+\infty$ to r_c, respectively. In the following, we shall assume that neither K^- nor K^+ is zero or infinite.

When $|r - r_c| = O(Re^{-1/6})$, pressure correction terms become of the same order as p_0 which indicates that we enter the Outer Viscous region.

3.3 Outer Viscous regions ($OV^{\pm}$)

The form of the solution in the two Outer Viscous regions is the same as for center modes. In these regions, the perturbation varies on the characteristic scale $\bar{r} = Re^{1/6}(r - r_c)$. Viscous effects become important such that the pressure fluctuations now depend on six independent solutions which have the following WKBJ approximation:

$$\bar{p} \sim Re^{-1/3}\bar{p}_2(\bar{r})\exp\left(Re^{1/6}\bar{\phi}(\bar{r})\right). \tag{16}$$

where $\bar{\phi}(\bar{r}) = \int_0^{\bar{r}} \mu$ with

$$\mathcal{L}(\mu, \omega_1, \bar{r}) \equiv \mu^2\left(\mu^2 + i\omega_1 - iK_c\frac{\bar{r}^2}{2}\right)^2 - H_c = 0, \tag{17}$$

and the constants H_c and K_c have been defined in (14). As for center modes, the first ring modes are obtained for ω_1 such that $\bar{r} = 0$ is a double turning point of the WKBJ approximation, that is $\mathcal{L}_\mu(\mu(0), \omega_1, \bar{r} = 0) = 0$. This provides the value of ω_1:

$$\omega_1 = 3i\left(\frac{H_c}{4}\right)^{1/3}. \tag{18}$$

As shown in LDF07, after rescaling, Eq. (17) with ω_1 given by (18) defines 6 different cases (K_c can be assumed positive), and as for center modes, 3 of them will provide eigenmodes. The six roots of (17) for the 6 different cases have been plotted in figure 2 of LDF07.

Here, we shall focus on the three eigenmode cases which corresponds, as in LDF07, when $K_c > 0$, to

$$\text{Mode A}: \ \omega_1 = \frac{3(\sqrt{3}+i)}{2}\left(\frac{-H_c}{4}\right)^{1/3}, \tag{19}$$

$$\text{Mode B}: \ \omega_1 = -3i\left(\frac{-H_c}{4}\right)^{1/3}, \tag{20}$$

when $H_c < 0$, and to

$$\text{Mode C}: \ \omega_1 = \frac{3(\sqrt{3}-i)}{2}\left(\frac{H_c}{4}\right)^{1/3}, \tag{21}$$

when $H_c > 0$.

The different solutions of (17) have been defined, as in LDF07, as follows: the branches $\mu^{(1)}$ and $\mu^{(2)} = -\mu^{(1)}$ correspond to the non-viscous branches which match with the behaviour near r_c of the ONV solutions $p^{(1)}$ and $p^{(2)}$ respectively. Contrarily to the 4 other viscous branches, the non-viscous branches go to zero as $|\bar{r}|$ goes to infinity. The branches $\mu^{(3)}$ and $\mu^{(4)}$ are such that they possess a negative real part for large $|\bar{r}|$. Thus, they are associated with viscous subdominant solutions in the ONV$^+$ region and dominant solutions in the ONV$^-$ region. The branch $\mu^{(3)}$ is in addition assumed to be equal to one of the non-viscous branches at $\bar{r} = 0$. For the 3 cases leading to eigenmode, $\mu^{(3)}(0) = \mu^{(1)}(0)$ while for the other cases $\mu^{(3)}(0) = \mu^{(2)}(0)$. The two other viscous branches are $\mu^{(5)} = -\mu^{(3)}$ and $\mu^{(6)} = -\mu^{(4)}$.

The condition of matching with a non-viscous solution in the ONV$^{\pm}$ regions imposes that $\mu^{(5)}$ and $\mu^{(6)}$ can not be part of the solution in the OV$^+$ region, and $\mu^{(3)}$ and $\mu^{(4)}$ can not be part of the solution in the OV$^-$ region. Moreover, the branches $\mu^{(4)}$ and $\mu^{(6)}$ are not connected to any other branch. So, if one of them is present in one the two regions, it is also present on the other Outer Viscous region, which is forbidden. For this reason, the general solution in the ONV$^{\pm}$ regions can be written as follows:

$$\begin{aligned}
\bar{p}^+ &\sim Re^{-1/3}\left[\bar{A}^{(1)+}\bar{p}_2^{(1)}e^{Re^{1/6}\bar{\phi}^{(1)}} + \bar{A}^{(2)+}\bar{p}_2^{(2)}e^{Re^{1/6}\bar{\phi}^{(2)}} + \bar{A}^{(3)+}\bar{p}_2^{(3)}e^{Re^{1/6}\bar{\phi}^{(3)}}\right] \text{ in } OV^+ \\
\bar{p}^- &\sim Re^{-1/3}\left[\bar{A}^{(1)-}\bar{p}_2^{(1)}e^{Re^{1/6}\bar{\phi}^{(1)}} + \bar{A}^{(2)-}\bar{p}_2^{(2)}e^{Re^{1/6}\bar{\phi}^{(2)}} + \bar{A}^{(5)-}\bar{p}_2^{(5)}e^{Re^{1/6}\bar{\phi}^{(3)}}\right] \text{ in } OV-
\end{aligned} \tag{22}$$

As shown in LDF07, the amplitude $\bar{p}_2$ for each solution is obtained by considering the problem at higher order. We obtain a similar equation for $\bar{p}_2$ as for center modes:

$$\mathcal{L}_\mu \frac{d\bar{p}_2}{d\bar{r}} + \left(\frac{1}{2}\mu'\mathcal{L}_{\mu\mu} + \frac{1}{2}\mathcal{L}_{\mu\bar{r}} + \mathcal{L}_{\omega_1}\omega_2 + \mathcal{H}\right)\bar{p}_2 = 0, \tag{23}$$

where the functions $\mathcal{L}_\mu$, $\mathcal{L}_{\mu\mu}$, $\mathcal{L}_{\mu\bar{r}}$ and $\mathcal{L}_{\omega_1}$ denote partial derivatives of $\mathcal{L}$ [defined in (17)] with respect to the indexes and taken at $(\mu, \omega_1, \bar{r})$ except for the operator $\mathcal{H}$ which is slightly different from the expression given in LDF07:

$$\mathcal{H} = -2iK_c\bar{r}\left(\mu^2 + i\omega_1 - iK_c\frac{\bar{r}^2}{2}\right)\mu. \tag{24}$$

It follows that

$$\bar{p}_2(\bar{r}) = \frac{1}{\sqrt{\mathcal{L}_\mu}}\exp\left(-\int^{\bar{r}}\frac{\omega_2\mathcal{L}_{\omega_1} + \mathcal{H}}{\mathcal{L}_\mu}\right), \tag{25}$$

such that if we compare with the pressure amplitude of the equivalent center mode we have $\bar{p}_2^{ring}(\bar{r}) = \sqrt{\bar{r}}\,\bar{p}_2^{\text{center}}$.

The behaviour of the solution towards the Intermediate region, that is as $|\bar{r}| \to 0$, is obtained as for center modes. The behaviour of the phase $\bar{\phi}$ for the eigenmodes satisfies as $|\bar{r}| \to 0$

$$\bar{\phi}^{(1)}(|\bar{r}|) = -\bar{\phi}^{(1)}(-|\bar{r}|) \sim \mu_0|\bar{r}| + G_0\bar{r}^2/4 \tag{26}$$

$$\bar{\phi}^{(2)}(|\bar{r}|) - \bar{\phi}^{(2)}(-|\bar{r}|) \sim -\mu_0|\bar{r}| - G_0\bar{r}^2/4 \tag{27}$$

$$\bar{\phi}^{(3)}(|\bar{r}|) \sim \mu_0|\bar{r}| - G_0\bar{r}^2/4 \tag{28}$$

$$\bar{\phi}^{(5)}(-|\bar{r}|) \sim -\mu_0|\bar{r}| + G_0\bar{r}^2/4 \tag{29}$$

where

$$\mu_0 = \mu_0^{(1)}(0) = \left(\frac{|H_c|}{4}\right)^{1/6}e^{i\gamma_0^{(1)}}, \quad G_0 = \partial_{\bar{r}}\mu_0^{(1)}(0)/2 = \left[\frac{2|K_c|}{3}\right]^{1/2}e^{i\pi/4}. \tag{30}$$

The angle $\gamma_0^{(1)}$ is $5\pi/6$, $-\pi/2 - \pi/3$ for modes A, B and C respectively. The normalisation of the amplitude $\bar{p}_2$ can be chosen such that $\bar{p}_2(\bar{r})$ expands as $|\bar{r}| \to 0$ as

$$\bar{p}_2^{(1)}(|\bar{r}|) = \bar{p}_2^{(2)}(-|\bar{r}|) \sim |\bar{r}|^{-1/2-\alpha} \tag{31}$$

$$\bar{p}_2^{(2)}(|\bar{r}|) = \bar{p}_2^{(1)}(-|\bar{r}|) \sim |\bar{r}|^{-1/2+\alpha} \tag{32}$$

$$\bar{p}_2^{(3)}(|\bar{r}|) \sim |\bar{r}|^{-1/2+\alpha} \tag{33}$$

$$\bar{p}_2^{(5)}(-|\bar{r}|) \sim |\bar{r}|^{-1/2-\alpha} \tag{34}$$

with

$$\alpha = \frac{\omega_2 e^{3i\pi/4}}{\sqrt{6|K_c|}}. \tag{35}$$

Gathering all the results, we finally obtain the behaviour of the OV^+ and OV^- solutions as $|\bar{r}| \to 0$:

$$\bar{p}^+ \sim Re^{-1/3}\bar{r}^{-1/2+\alpha}\left[\bar{A}^{(2)+}\mathrm{e}^{Re^{1/6}\left(-\mu_0|\bar{r}|-G_0\bar{r}^2/4\right)} + \bar{A}^{(3)+}\mathrm{e}^{Re^{1/6}\left(+\mu_0|\bar{r}|-G_0\bar{r}^2/4\right)}\right] + Re^{-1/3}\bar{r}^{-1/2-\alpha}\bar{A}^{(1)+}\mathrm{e}^{Re^{1/6}\left(\mu_0|\bar{r}|+G_0\bar{r}^2/4\right)}, \tag{36}$$

$$\bar{p}^- \sim Re^{-1/3}\bar{r}^{-1/2+\alpha}\left[\bar{A}^{(1)-}\mathrm{e}^{Re^{1/6}\left(-\mu_0|\bar{r}|-G_0\bar{r}^2/4\right)} + \bar{A}^{(5)-}\mathrm{e}^{Re^{1/6}\left(+\mu_0|\bar{r}|-G_0\bar{r}^2/4\right)}\right] + Re^{-1/3}\bar{r}^{-1/2-\alpha}\bar{A}^{(2)-}\mathrm{e}^{Re^{1/6}\left(\mu_0|\bar{r}|+G_0\bar{r}^2/4\right)}, \tag{37}$$

The matching with the $\mathrm{ONV}^\pm$ solutions provides a condition between the coefficients. The two subdominant viscous branches $\mu^{(3)}$ and $\mu^{(5)}$ become negligible as $|\bar{r}|$ goes to infinity. The two other non-viscous branches are matched to the non-viscous solutions of the $\mathrm{ONV}^\pm$ regions. For the normalisation chosen above, $\bar{p}_2$ is such that for large $|\bar{r}|$ we have

$$p_2^{(1)}(|\bar{r}|) = p_2^{(2)}(-|\bar{r}|) \sim \bar{C}_\infty^{(1)}|\bar{r}|, \quad p_2^{(2)}(\bar{r}) = p_2^{(1)}(-|\bar{r}|) \sim \bar{C}_\infty^{(2)}|\bar{r}|, \tag{38}$$

where $\bar{C}_\infty^{(1)}$ and $\bar{C}_\infty^{(2)}$ are constants. If we define $\bar{\phi}_\infty^{(1)} = \int_0^\infty \mu^{(1)}$, the conditions of matching reduce to

$$A_\infty^+ = \bar{A}^{(1)+}\bar{C}_\infty^{(1)}Re^{1/12}\mathrm{e}^{Re^{1/6}\bar{\phi}_\infty^{(1)}}, \quad B_\infty^+ = \bar{A}^{(2)+}\bar{C}_\infty^{(2)}Re^{1/12}\mathrm{e}^{-Re^{1/6}\bar{\phi}_\infty^{(1)}}, \tag{39}$$

$$A_\infty^- = \bar{A}^{(1)-}\bar{C}_\infty^{(2)}Re^{1/12}\mathrm{e}^{-Re^{1/6}\bar{\phi}_\infty^{(1)}}, \quad B_\infty^- = \bar{A}^{(2)-}\bar{C}_\infty^{(1)}Re^{1/12}\mathrm{e}^{Re^{1/6}\bar{\phi}_\infty^{(1)}}. \tag{40}$$

It follows that the ratios of the amplitudes of the two $\mathrm{ONV}^\pm$ solutions are

$$\frac{\bar{A}^{(1)+}}{\bar{A}^{(2)+}} = K^+\frac{\bar{C}_\infty^{(1)}}{\bar{C}_\infty^{(2)}}\exp(-2Re^{1/6}\bar{\phi}_\infty^{(1)}), \quad \frac{\bar{A}^{(1)-}}{\bar{A}^{(2)-}} = K^-\frac{\bar{C}_\infty^{(2)}}{\bar{C}_\infty^{(1)}}\exp(2Re^{1/6}\bar{\phi}_\infty^{(1)}). \tag{41}$$

As explained in LDF07, for the eigenmodes, $\Re e(\phi_\infty^{(1)}) > 0$ which implies that $\bar{A}^{(1)+}$ is exponentially small compared to $\bar{A}^{(2)+}$, and $\bar{A}^{(2)-}$ is exponentially small compared to $\bar{A}^{(1)-}$.

3.4 Intermediate region $|r - r_c| = O(Re^{-1/4})$

In this region, the pressure fluctuation varies on the scale $\tilde{r} = Re^{1/4}(r - r_c) = Re^{1/12}\bar{r}$ and can be written as:

$$\tilde{p} \sim \tilde{p}_4^+(\tilde{r})\exp\left(Re^{1/12}\mu_0\tilde{r}\right) + \tilde{p}_4^-(\tilde{r})\exp\left(-Re^{1/12}\mu_0\tilde{r}\right). \tag{42}$$

Using the same approach as in LDF07, we obtain an equation for $\tilde{p}_4^\pm$ which reads:

$$[(\tilde{\Delta} + i\tilde{\Phi})\hat{\Delta}(\tilde{\Delta} + i\tilde{\Phi}) - H_c]\tilde{p}_4^\pm = 0, \tag{43}$$

where

$$\tilde{\Phi} = \omega_1 + Re^{-1/6}\left(\omega_2 - K_c\frac{\tilde{r}^2}{2}\right), \quad \tilde{\Delta} = \mu_0^2 + Re^{-1/12}2\mu_0\frac{\partial}{\partial\tilde{r}} + Re^{-1/6}\frac{\partial^2}{\partial\tilde{r}^2}. \tag{44}$$

From this equation, we deduce at the order $Re^{-1/6}$

$$\left(\frac{\partial^2}{\partial\tilde{r}^2} + \frac{i\omega_2}{3} - iK_c\frac{\tilde{r}^2}{6}\right)\tilde{p}_4^\pm = 0, \tag{45}$$

which can be also written as

$$\left(\frac{\partial^2}{\partial x^2} + \alpha - \frac{x^2}{4}\right)\tilde{p}_4^\pm = 0, \tag{46}$$

if we use the above definition (35) of α and

$$x = \left[\frac{2|K_c|}{3}\right]^{1/4} \mathrm{e}^{i\pi/8}\tilde{r}. \tag{47}$$

Equation (45) is a parabolic cylinder equation [2] which possesses two independent solutions $D_{\alpha-1/2}(x)$, and $D_{\alpha-1/2}(-x)$. The condition of matching with the OV$^{\pm}$ regions imposes that only one of them is present in each solution such that we obtain

$$\tilde{p} = \tilde{A}^{+} D_{\alpha-1/2}(-x)\mathrm{e}^{+Re^{1/12}\mu_0\tilde{r}} + \tilde{A}^{-} D_{\alpha-1/2}(x)\mathrm{e}^{-Re^{1/12}\mu_0\tilde{r}}, \tag{48}$$

where $\tilde{A}^{+}$ and $\tilde{A}^{-}$ are constants.

3.5 Matching and frequency selection

The matching between Intermediate and Outer Viscous regions is performed using the asymptotic expansions of the parabolic cylinder solution as $|x| \to \infty$ [2]:

$$D_\nu(x) \sim x^\nu \mathrm{e}^{-x^2/4},\ |\arg(x)| < 3\pi/4,$$
$$D_\nu(x) \sim x^\nu \mathrm{e}^{-x^2/4} - \frac{\sqrt{2\pi}}{\Gamma(-\nu)} \mathrm{e}^{i\pi\nu} x^{-\nu-1} \mathrm{e}^{x^2/4},\quad \pi/4 < \arg(x) < 5\pi/4.$$

The intermediate solution behaves for large $|\tilde{r}|$ as

$$\tilde{p} \underset{\tilde{r}\to+\infty}{\sim} \left(G_0^{1/4} Re^{1/12}|\bar{r}|\right)^{\alpha-1/4} \left(-i\tilde{A}^{+}\mathrm{e}^{i\pi\alpha}\mathrm{e}^{Re^{1/6}(\mu_0|\bar{r}|-G_0\frac{\bar{r}^2}{4})} + \tilde{A}^{-}\mathrm{e}^{Re^{1/6}(-\mu_0|\bar{r}|-G_0\frac{\bar{r}^2}{4})}\right)$$
$$+ \frac{\sqrt{2\pi}}{\Gamma(-\alpha+1/2)} \left(G_0^{1/4} Re^{1/12}\bar{r}\right)^{-\alpha-1/2} \tilde{A}^{+}\mathrm{e}^{Re^{1/6}(\mu_0|\bar{r}|+G_0\frac{\bar{r}^2}{4})} \tag{49}$$

$$\tilde{p} \underset{\tilde{r}\to-\infty}{\sim} \left(G_0^{1/4} Re^{1/12}|\bar{r}|\right)^{\alpha-1/2} \left(\tilde{A}^{+}\mathrm{e}^{Re^{1/6}(-\mu_0|\bar{r}|-G_0\frac{\bar{r}^2}{4})} - i\tilde{A}^{-}\mathrm{e}^{i\pi\alpha}\mathrm{e}^{Re^{1/6}(\mu_0|\bar{r}|-G_0\frac{\bar{r}^2}{4})}\right)$$
$$+ \frac{\sqrt{2\pi}}{\Gamma(-\nu)} \left(G_0^{1/4} Re^{1/12}|\bar{r}|\right)^{-\nu-1} \tilde{A}^{-}\mathrm{e}^{Re^{1/6}(\mu_0|\bar{r}|+G_0\frac{\bar{r}^2}{4})} \tag{50}$$

where α and G_0 have been defined in (30) and (35), respectively. Comparing the above expansions with (36) and (37) leads to the relations:

$$\tilde{A}^{+} G_0^{\alpha/4-1/8} Re^{\alpha/12-1/24} = \bar{A}^{(1)-} = i\bar{A}^{(3)+}\mathrm{e}^{-i\pi\alpha}; \tag{51}$$
$$\tilde{A}^{-} G_0^{\alpha/4-1/8} Re^{\alpha/12-1/24} = \bar{A}^{(2)+} = i\bar{A}^{(5)-}\mathrm{e}^{-i\pi\alpha}; \tag{52}$$
$$\tilde{A}^{+} G_0^{-\alpha/4-1/8} Re^{-\alpha/12-1/24} \frac{\sqrt{2\pi}}{\Gamma(-\alpha+1/2)} = \bar{A}^{(1)+}; \tag{53}$$
$$\tilde{A}^{-} G_0^{-\alpha/4-1/8} Re^{-\alpha/12-1/24} \frac{\sqrt{2\pi}}{\Gamma(-\alpha+1/2)} = \bar{A}^{(2)-}, \tag{54}$$

from which we deduce using (41)

$$\frac{2\pi G_0^{-\alpha}}{(\Gamma(-\alpha+1/2))^2} Re^{-\alpha/3} = \frac{\bar{A}^{(1)+}\bar{A}^{(2)-}}{\bar{A}^{(2)+}\bar{A}^{(1)-}} = \frac{K^{+}}{K^{-}} \left(\frac{\bar{C}_\infty^{(1)}}{\bar{C}_\infty^{(2)}}\right)^2 \exp(-4Re^{1/6}\bar{\phi}_\infty^{(1)}). \tag{55}$$

Since $\Re e(\bar{\phi}_\infty^{(1)}) > 0$, the above equation implies that, for large Re, $1/\Gamma(-\alpha+1/2)$ is very small, which means that $\alpha - 1/2$ is close to a positive integer n. Using the asymptotic expansion:

$$\frac{1}{\Gamma(-\nu)} \underset{\nu\to n}{\sim} -(-1)^n n!(\nu - n) \tag{56}$$

we obtain

$$\alpha \sim n + \frac{1}{2} \pm G_n Re^{n/6+1/12} \exp(-2Re^{1/6}\bar{\phi}_\infty^{(1)}) \tag{57}$$

where G_n is a numerical constant:

$$G_n = \frac{G_1^{2n+1}}{n!\sqrt{2\pi}} \sqrt{\frac{K^+}{K^-}} \frac{\bar{C}_\infty^{(1)}}{\bar{C}_\infty^{(2)}}. \tag{58}$$

We finally deduce the value of the second order frequency ω_2:

$$\omega_2 = \sqrt{6|K_c|} e^{-3i\pi/4} \left(n + \frac{1}{2} \pm G_n Re^{n/6+1/12} \exp(-2Re^{1/6}\bar{\phi}_\infty^{(1)}) \right) \quad \text{with} \quad n = 0, 1, 2, 3, \ldots \tag{59}$$

4 Ring modes characteristics

4.1 Characteristics of the eigenmodes

As for center modes, the above analysis provides three families of ring modes corresponding to the three different values of the first order frequency correction ω_1 defined in (19)–(21). In fact, for given values of H_c and K_c, there exist two families (modes A and modes B) when $H_c < 0$ and one family (modes C) when $H_c > 0$. Only the modes A for which $\Im m(\omega_1) > 0$ are unstable. Contrarily to center modes, ring modes in each family come by pair. This duplicity is visible in formula (59) for ω_2: for each n, there are two second order frequency corrections defining two different modes. This in particular means that there are twice more ring modes that center modes. Formula (59) also tells us that the frequency separation of the two modes in each pair is a priori exponentially small and depends on the index n. It also depends on the characteristics of the ONV$^\pm$ solutions via the coefficients K^+ and K^- in G_n. These coefficients intervene also in the definition of the eigenmodes in the different regions, which renders the approximation of the eigenmode in principle more complicated. However, it was shown in LDF07 that center modes A are mainly localized in the Outer Viscous region and well described by a simple WKBJ approximation. The same result is true for ring modes A because they have the same structure as center modes in the Outer Viscous regions. As in LDF07, expression (22) can be reduced to a single term, and if we do not consider the amplitude term, it takes the form of a geometrical optics approximation:

$$p \approx \exp\left(Re^{1/6} \eta \Lambda^{(2)}(\gamma Re^{1/6}|r - r_c|) \right) \tag{60}$$

where

$$\eta = 3\sqrt{\frac{2}{|K_c|}} \left| \frac{H_c}{4} \right|^{1/3}, \quad \gamma = \sqrt{\frac{|K_c|}{6}} \left| \frac{4}{H_c} \right|^{1/6}, \tag{61}$$

and $\Lambda^{(2)}$ is an universal complex function plotted in Fig. 2. The function $\Lambda^{(2)}$ was already plotted in figure 5(a) of LDF07. This approximation a priori applies in the two OV$^\pm$ regions of the ring modes. However, in practice, it turns out that the modes are large in one of the two regions only. In principle, one could determine the region where each mode is the largest by computing the coefficients K^+ and K^- and the amplitude factors. But for the comparisons which will be made below, we shall not try to do that but instead use the above approximation in the region where the mode is localized.

4.2 Instability criterion

Unstable ring modes exist only if $H_c < 0$ and the leading order growth rate of the most unstable ring mode is

$$\sigma = Re^{-1/3} \frac{3}{2} \left| \frac{H_c}{4} \right|^{1/3}. \tag{62}$$

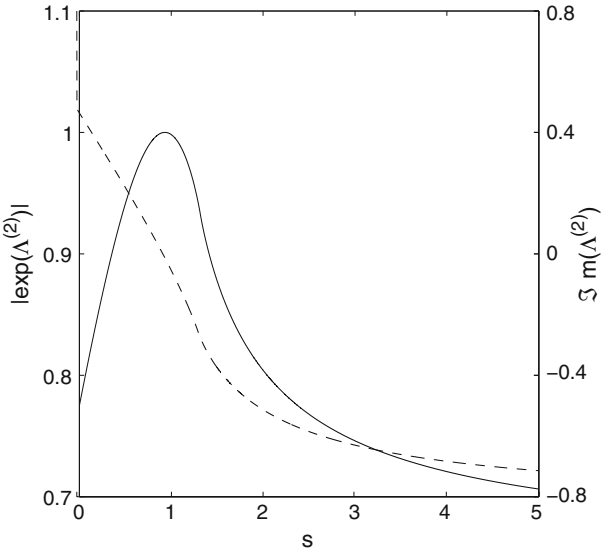

Fig. 2 Characteristics of the function $\Lambda^{(2)}$. *Solid line*: $|\exp(\Lambda^{(2)}(s))|$ versus s. *Dashed line*: $\Im m(\Lambda^{(2)}(s))$ versus s

The condition of instability together with the double critical point condition $m\Omega_c' + kW_c' = 0$ implies that we should have at r_c:

$$\Omega_c\Omega_c'[r_c\Omega_c'(2\Omega_c + r_c\Omega_c') + (W_c')^2] < 0. \tag{63}$$

Inversely, if (63) is satisfied at any point r_c and if at that location $W_c' \neq 0$ then, for any $m \neq 0$, there exists a wavenumber k, given by $k = -m\Omega_c'/W_c'$ which guarantees that r_c is a double critical point for the frequency $\omega = m\Omega_c + kW_c$. Thus the above analysis can be performed which means that there exist unstable ring modes A if the Reynolds number is sufficiently large. Note in particular that unstable ring modes require axial flow and swirl. If $W = 0$, the double critical point condition requires $\Omega_c' = 0$ which implies $H_c = 0$, thus stability.

For inviscid ring modes, we have the same condition of instability for the large azimuthal wavenumbers [7]: we should have (63) and $W_c' \neq 0$. In particular, these modes are also stable if $W = 0$. However, the axisymmetric mode $m = 0$, associated with the centrifugal instability is unstable for $W = 0$ as soon as (63) is satisfied. This mode can also be considered as a ring mode in the limit of large k but instead of being localized near a double critical point, the most unstable centrifugal mode is localized near the minimum of the Rayleigh discriminant $\Phi = 2\Omega(r)\Xi(r)$.

The leading order growth rate of inviscid ring modes is [7] $\sigma \sim \sqrt{r_c^2/(m^2 + k^2r_c^2)}\sqrt{-H_c}$. As this growth rate does not depend on the Reynolds number, inviscid ring modes are then expected to be more unstable than viscous ring modes, when $H_c < 0$, if the Reynolds number is sufficiently large. However, this is not guaranteed for all Reynolds numbers. Indeed, the growth rate of inviscid ring modes is the largest for large m, but it is also for large m that the damping associated with viscosity is the largest. Close to the curve $H_c = 0$, the leading order growth rate of both types of ring modes vanishes. It is therefore near such a marginal curve that we expect the competition and the interplay of viscous and non-viscous modes to become important. The analysis of that marginal curve has been performed for center modes in Fabre and Le Dizès [4]. It was shown that near that curve, the initial three-zone structure can be reduced to a single one-zone problem. Unfortunately, such an analysis cannot be performed the same way for ring modes, because the structure of the asymptotic problem remains complex, with the same number of zones that in the present analysis. The analysis of the marginal curve and of the competition between viscous and inviscid ring modes is then left for future works.

5 Application to the q-vortex model

The q-vortex model (also called Batchelor vortex) is defined by

$$\Omega(r) = q\frac{1 - \exp(-r^2)}{r^2}; \quad W(r) = \exp(-r^2), \tag{64}$$

where q is the so-called swirl parameter.

For this vortex, the condition (63) for the instability of ring modes is $q < \sqrt{2}$. In fact, for any negative azimuthal wavenumber m, ring modes are unstable in the (q, k) domain delimited by the curves

$$k > -mq/2, \quad q > 0, \quad k < -m/q, \tag{65}$$

and which has been sketched in Fig. 3 for $m = -1$. The left and upper marginal curves correspond to the vanishing of H_c. On these curves the above analysis breaks down. The lower curve is associated with the transformation of ring modes into center modes: the point r_c is at the origin on this line. On this line, H_c does not vanish but the analysis breaks down because $K_c = 0$. Below this line, there is no double critical point different from the origin.

In Fig. 3 is also indicated the instability domain of viscous center modes [6]. This domain includes and is larger than the ring mode instability domain. The leading order growth rate of both types of modes is given by $Re^{-1/3}(3/2)(|H(r)|/4)^{1/3}$ with $r = 0$ for center modes and $r = r_c$ for ring modes where the function $H(r)$ is given by

$$H(r) = 4q\frac{(1 - e^{-r^2})}{r^2}e^{-r^2}(kq + m). \tag{66}$$

The function $|H(r)|$ is strictly decreasing, which means that for the q-vortex model, ring modes are always less unstable than center modes.

The spectrum obtained by numerical integration of the eigenvalue problem is plotted in Fig. 4 for a particular example. The code is the same as the one used in LDF07. The chosen parameters correspond to the point indicated by a diamond in Fig. 3. For these parameters, there are no unstable inviscid modes but there exist unstable viscous ring modes and unstable viscous center modes, close to the frequencies $\omega_0 \approx -0.026$ and $\omega_0 \approx 2.3$ respectively. For both modes, we have compared the numerical spectrum to the asymptotic predictions (see the close-up views). For center modes, we have used the asymptotic formula obtained in Le Dizès and Fabre [6]. For ring modes, we have used the formula obtained in the previous section but we

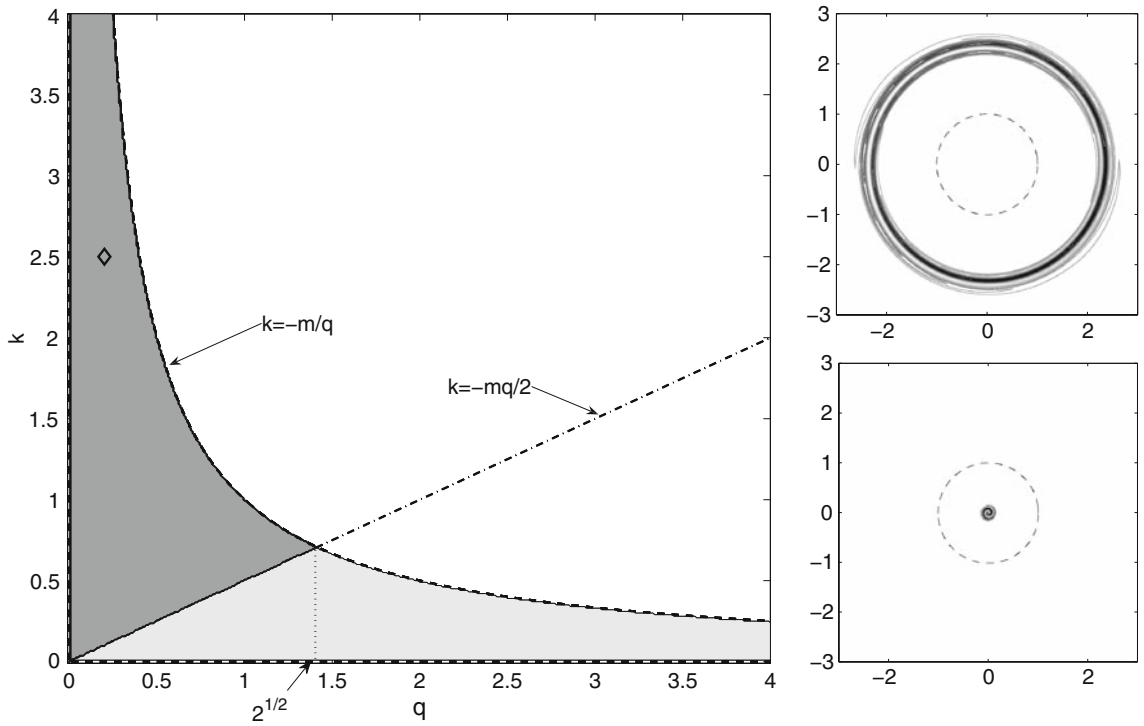

Fig. 3 *Left*: Domain of instability of viscous ring modes (dark gray region) and viscous center modes (dark and light gray regions) in the limit of large Reynolds numbers, here plotted for $m = -1$. *Right*: The axial vorticity field of the most unstable ring mode (*top*) and the most unstable center mode (*bottom*) for the parameters indicated by a diamond on the left graph and for $Re = 10^6$. The vortex core size is visualized by the dashed circle. More information on the spectrum and the modes for these parameters are also found in Figs. 4 and 5

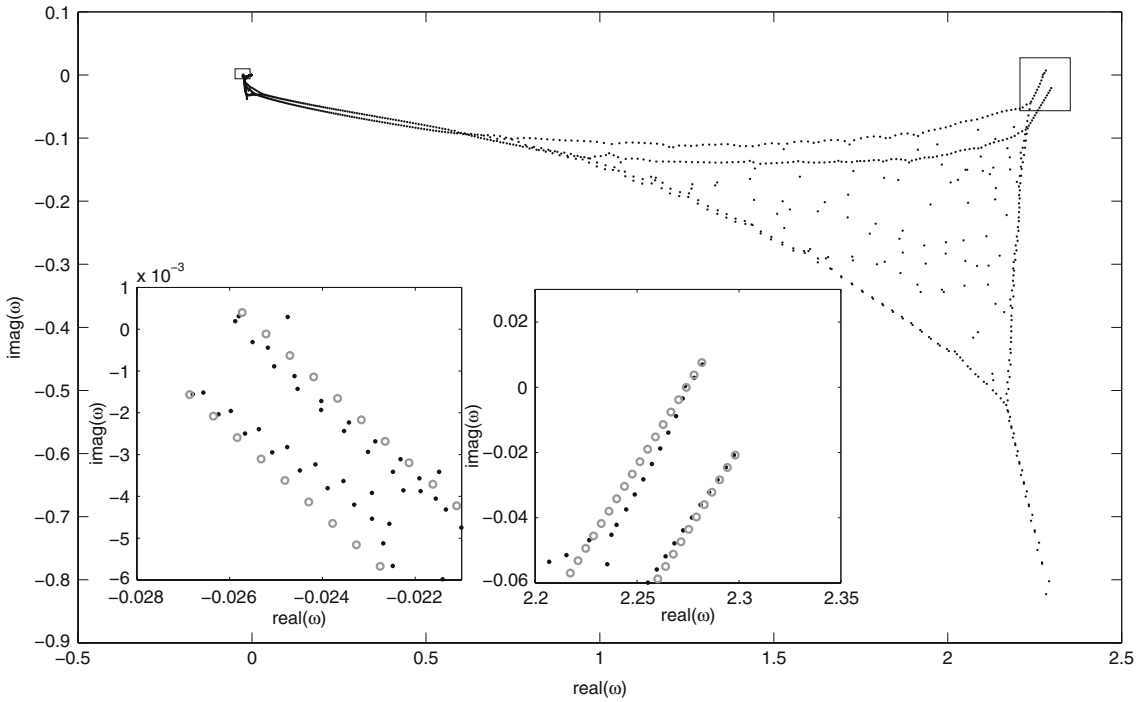

Fig. 4 Temporal spectrum of the q-vortex model for $q = 0.2$, $Re = 10^6$, $m = -1$ and $k = 2.5$, obtained by a numerical spectral code with $N = 600$ polynomials. Close-up views: comparison with the theory for ring modes (*left*) and for center modes (*right*)

have taken $G_n = 0$ in formula (59) for simplicity. This simplification means that we have not separated the two ring modes obtained for each value of n. For both center and ring modes, modes A and modes B have been obtained. We can notice that the agreement between theory and numerics is good for both center modes and ring modes. Note in particular that there are indeed twice more ring modes than center modes in each mode family. The main frequency correction ω_1 is correctly predicted as well as the spacing between consecutive frequencies.

The spatial structure of the 3 most unstable ring modes is displayed in Fig. 5a,b and c. These modes are modes A. As expected from the theory, the structure of these modes are similar and concentrated in the neighborhood of the critical point r_c. Figure 5d demonstrates that this structure is very well described by the geometrical optics approximation (60) of mode A in the Outer Viscous region. It is worth mentioning that there are no free parameters in this comparison albeit the adimensionalisation: the structure is normalized such that the pressure is equals to 1 at its maximum amplitude. The above agreement for both the frequency and the spatial structure of the ring modes is a strong validation of the theory.

6 Conclusion

In this article, we have demonstrated the existence of three families of viscous ring modes localized in the neighborhood of a double critical point. We have shown that one family (modes A) provides unstable modes for sufficiently large Reynolds numbers as soon as there exist a point r_c where

$$\Omega_c \Omega_c' [r_c \Omega_c' (2\Omega_c + r_c \Omega_c') + (W_c')^2] < 0$$

and $W_c' \neq 0$. We have obtained an explicit expression for the frequency of the modes as well as a simple approximation for the unstable modes. The frequency prediction and the mode approximation have been tested with respect to numerical results for the q-vortex model and a good agreement has been demonstrated.

We have shown that for the q-vortex model, the viscous ring modes are always less unstable than center modes. This is not always the case for all vortices. For example, a vortex with the following angular and axial velocity profiles:

$$\Omega(r) = q r^2 \mathrm{e}^{-r^2}, \quad W(r) = r^4 \mathrm{e}^{-r^2}, \tag{67}$$

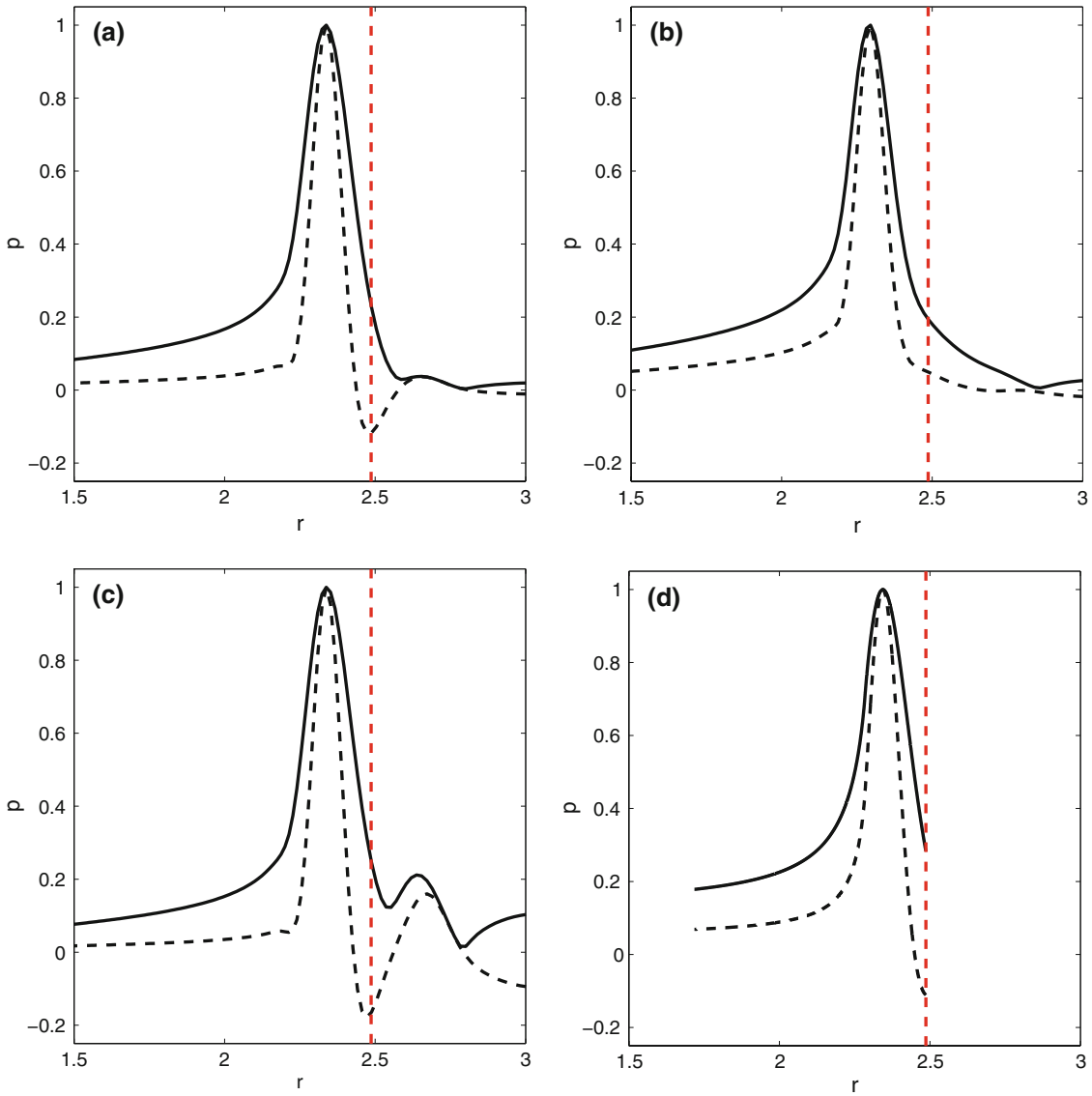

Fig. 5 Spatial structure (real part in *dashed line*, and modulus in *solid line*) of the most unstable viscous ring modes of the q-vortex model for $q = 0.2$, $Re = 10^6$, $m = -1$ and $k = 2.5$. **a,b,c** numerical results for the three most unstable modes. **d** geometrical optics approximation (60) of the ring mode A. The vertical dashed line indicates the position of the critical point r_c

does not possess unstable viscous center modes but exhibits unstable viscous ring modes. However, as mentioned above, these viscous ring modes are always in competition with inviscid modes. It will be interesting to analyse the competition between both modes for weakly unstable profiles or in the neighborhood of the marginal curves.

Acknowledgments This work has been supported by the European community (Far-WAKE project) and the French research agency (VORTEX Project).

References

1. Ash, R.L., Khorrami, M.R.: Vortex stability. In: Green, S.I. (ed.) Fluid Vortices, chap. VIII, pp. 317–372. Kluwer, Dordrecht (1995)
2. Bender, C.M., Orszag, S.A.: Advanced Mathematical Methods for Scientists and Engineers. McGraw-Hill, New York (1978)
3. Fabre, D., Jacquin, L.: Viscous instabilities in trailing vortices at large swirl numbers. J. Fluid Mech. **500**, 239–262 (2004)

4. Fabre, D., Le Dizès, S.: Viscous and inviscid centre modes in the linear stability of vortices: the vicinity of the neutral curves. J. Fluid Mech. **603**, 1–38 (2008)
5. Heaton, C.: Centre modes in inviscid swirling flows, and their application to the stability of the Batchelor vortex. J. Fluid Mech. **576**, 325–348 (2007)
6. Le Dizès, S., Fabre, D.: Large-Reynolds-number asymptotic analysis of viscous centre modes in vortices. J. Fluid Mech. **585**, 153–180 (2007)
7. Leibovich, S., Stewartson, K.: A sufficient condition for the instability of columnar vortices. J. Fluid Mech. **126**, 335–356 (1983)
8. Stewartson, K.: The stability of swirling flows at large Reynolds number when subjected to disturbances with large azimuthal wavenumber. Phys. Fluids **25**, 1953–1957 (1982)
9. Stewartson, K., Ng, T.W., Brown, S.N.: Viscous centre modes in the stability of swirling Poiseuille flow. Phil. Trans. R. Soc. Lond. A **324**, 473–512 (1988)